

Spatial separation of vacancy and interstitial defects formed in Si by oxygen-ion irradiation at elevated temperature

I. Danilov, H. Boudinov, J. P. de Souza, and Yu. N. Drozdov

Citation: [Journal of Applied Physics](#) **97**, 076106 (2005); doi: 10.1063/1.1886269

View online: <http://dx.doi.org/10.1063/1.1886269>

View Table of Contents: <http://scitation.aip.org/content/aip/journal/jap/97/7?ver=pdfcov>

Published by the [AIP Publishing](#)



Re-register for Table of Content Alerts

Create a profile.



Sign up today!



Spatial separation of vacancy and interstitial defects formed in Si by oxygen-ion irradiation at elevated temperature

I. Danilov, H. Boudinov,^{a)} and J. P. de Souza^{b)}

Instituto de Física, Universidade Federal do Rio Grande do Sul, Porto Alegre, Rio Grande do Sul 91501-970, Brazil

Yu. N. Drozdov

Institute for Physics of Microstructures, Russian Academy of Sciences, Nizhny Novgorod 603600, Russia

(Received 18 October 2004; accepted 10 February 2005; published online 29 March 2005)

A study of damage depth distribution in Si by elevated temperature O⁺-ion implantation was performed using three structures: (i) bulk Si, (ii) Si/SiO₂/bulk Si, and (iii) SiO₂/bulk Si. The samples were implanted at 250 °C with a dose of 5×10^{16} cm⁻² at an energy of 185 keV. By this approach, the damage depth profile distributes along the SiO₂ and Si layers in a different manner according to the sample structure. A comparative analysis of the high-resolution x-ray diffraction spectra taken from the implanted samples permitted us to infer on the spatial separation between vacancy and interstitial-rich layers, which are associated with the presence of negative and positive strained layers, respectively. © 2005 American Institute of Physics. [DOI: 10.1063/1.1886269]

High-dose oxygen-ion implantation in Si at elevated temperatures is used for the synthesis of buried oxide layer in the method called separation by implanted oxygen (SIMOX). In the “standard” process O⁺-ion implantation is used with a dose of 1.8×10^{18} cm⁻² at a temperature of 590 °C, followed by thermal annealing in an Ar+O₂ mixture at 1320–1350 °C for many hours.¹ A successful SIMOX production technology² employs two O⁺ implants: the first implant performed at a high temperature ($T > 200$ °C) with doses $(2-4) \times 10^{17}$ cm⁻² and the second implant performed at room temperature with lower doses $(1-5) \times 10^{15}$ cm⁻².

In earlier works it was proposed that depth profiles of vacancy- and interstitial-type defects are spatially separated due to vacancy-interstitial recombination during high temperature implantation.^{3,4} One more precise explanation considers that spatial separation of defects from created Frenkel pairs occurs as a result of atomic displacement.⁵ The momentum transferred to the recoiled Si atom should have a non-zero component along the direction of the incident ion beam. On the average, this should lead to a spatial separation between the interstitial and vacancy depth distributions with the interstitials distributed to a greater depth. Up to now few works have been performed to observe this spatial separation. In these experimental works, light ions implanted at high energies^{6,7} or at low doses⁸ were considered. The technique of deep-level transient spectroscopy was applied^{6,8} to measure implantation-induced changes in vacancy- and interstitial-type defect concentrations. The interpretation of the obtained data is not straightforward and not completely conclusive.^{9,10} In addition, detailed information on the damage profiles in Si formed by high dose O⁺ implantation at elevated temperatures are not available yet.

We present a comparative study of internal strain forma-

tion in O⁺-implanted Si at high temperature in three different structures: a) bulk Si, b) SIMOX, and c) SiO₂/Si structure with a variable oxide thickness. The difference in x-ray diffraction spectra for these structures allows us to determine the spatial positions of vacancy- and interstitial-rich layers, which are associated with the presence of negatively and positively strained layers, respectively.

Czochralski-grown silicon wafers of *n*-type conductivity, with resistivity of 1–2 Ω cm and (100) orientation, were oxidized in dry O₂ to obtain SiO₂/Si structures with oxide thickness in the range of 50–230 nm. SIMOX samples with 200-nm Si overlayer and 400-nm-buried SiO₂ layer and bulk Si samples were used.

The samples were implanted with O⁺ ions at a temperature of 250 °C with a dose of 5×10^{16} cm⁻² at an energy of 185 keV. The ion-beam current density was maintained at ~ 5 μA/cm². To minimize channeling effects during the ion implantation, the normal to the sample surface was tilted by 7° with respect to the incident beam direction, and the surface rotated by 25° with respect to the ⟨110⟩ direction.

Internal mechanical strain was investigated by high-resolution x-ray diffraction (HRXRD) measurements in double-axis configuration using a Cu Kα₁ beam. By measuring the angular distance between the diffraction peaks from the Si substrate and the implanted layer in the (004) reflection rocking curves (RC), the relative perpendicular mismatch $(\Delta d/d)_{\perp}$ was obtained. The in-plane component of the strain was found to be negligible in all the cases, by examination of the reflections from the inclined lattice planes.

The interstitial-vacancy depth profiles were calculated using the binary-collision code MARLOWE.¹¹ It is a comprehensive computer program that has been developed for the simulation of atomic displacement in a variety of crystalline solids using the binary-collision approximation to determine the particle trajectories. The atomic scattering is governed by a screened potential, taking into account the temporal aspects of binary collisions.¹² This software gives a result of the

^{a)}Electronic mail: henry@if.ufrgs.br

^{b)}Present address: T. J. Watson Research Center, IBM, Yorktown Heights, NY, 10598.

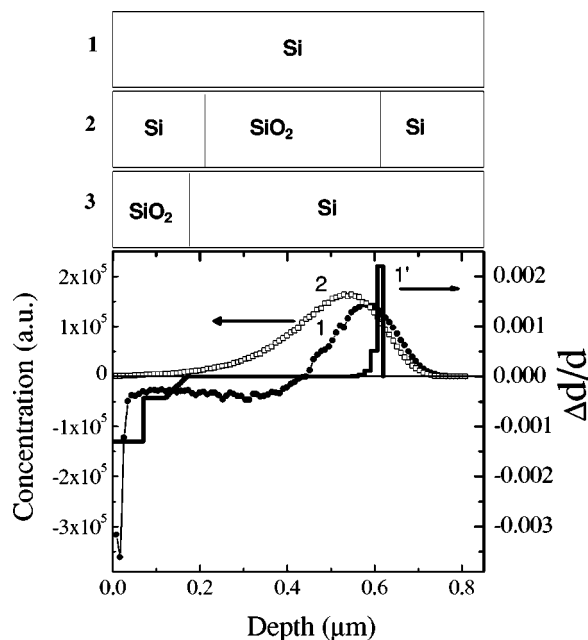


FIG. 1. Vacancy-interstitial excess concentration profile (curve 1) and oxygen depth distribution (curve 2), simulated by the MARLOWE code. Curve 1' represents the strain depth profile obtained by fitting to experimental RC. The implanted structures are shown on the top: (1) Si, (2) SIMOX, and (3) SiO₂/Si.

distributions of interstitials and vacancies separately.

Figure 1 shows the main idea of this work. The curve with full circles represents the calculated vacancy-interstitial excess concentration profile. Negative values of this distribution, from the surface up to $\sim 0.4 \mu\text{m}$, correspond to a layer with an excess vacancy concentration. The positive values at depths of $\sim 0.5\text{--}0.7 \mu\text{m}$ correspond to a layer with an interstitial excess concentration. The curve with open circles represents the calculated oxygen distribution. The structures used are shown on the top of Fig. 1: (1) Si, (2) SIMOX, and (3) 180-nm SiO₂/Si. X-ray diffraction technique represents difficulties on the determination of the depth position of a layer with the lattice parameter different from that of the matrix. Taking into account a similar stopping power of ions in Si and SiO₂, we can assume that the distributions of energy transmitted to nuclear collisions in depth scale are similar in the three structures used. But in amorphous material (SiO₂), the ion beam does not create any x-ray measurable defects. In this way we have separated the defect layers excluding the interstitial layer in the SIMOX and the near surface part of the vacancy layer in the SiO₂/Si structures.

In Fig. 2 are presented the (004) reflection rocking curves of the implanted structures. The RC of unimplanted Si (not shown) has only a narrow peak from substrate (004) reflection. The RC of implanted bulk Si [see curve (1)] displays large right and left shoulders of the main peak, indicating the existence of regions with negative and positive lattice strain, respectively. It was shown previously that ion implantation at elevated temperature and high doses produces a negatively strained layer (contraction strain) close to the sample surface, and the magnitude of negative strain depends on the dose, temperature, and chemical species of the implanted ion.^{13,14}

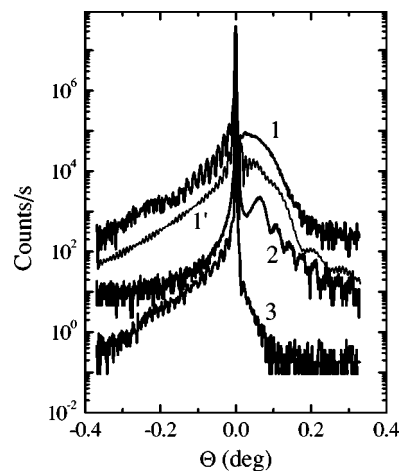


FIG. 2. X-ray (004) rocking curves from the structures implanted with 185-keV O⁺ ions at 250 °C with a dose of $5 \times 10^{16} \text{ cm}^{-2}$: (1) Si, (2) SIMOX, and (3) 180-nm SiO₂/Si. Curve 1' represents the RC, simulated with the strain profile as shown in Fig. 1.

The implanted SIMOX structure (Fig. 2, curve 2) has shown a RC with left shoulder similar to that of the unimplanted SIMOX (not shown). The principal changes are observed on the right shoulder of the RC. The strong fringes on the right shoulder indicate the existence of negative-strain region in ion-implanted SIMOX structure. But the shape of the left shoulder suggests that positive strain is absent.

Contrary to this case, the RC of implanted SiO₂-Si structure (Fig. 2, curve 3), having a 0.18- μm superficial SiO₂ film, represents practically not an appreciable right shoulder, and the left shoulder is similar to that of the implanted bulk Si (Fig. 2, curve 1).

Figure 3 shows the changes of the RCs for the implanted SiO₂-Si structures with a variable thickness (t_{ox}) of SiO₂ in the range of 0–230 nm. The intensity and broadening of the right shoulder, caused by the existence of region with negative strain, decrease monotonically. This shoulder disappears fully at $t_{\text{ox}}=230 \text{ nm}$.

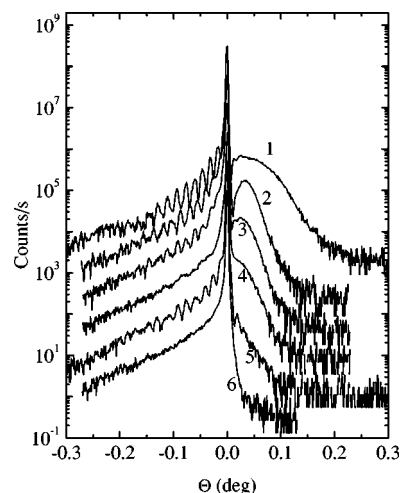


FIG. 3. X-ray rocking curves of implanted SiO₂/Si structures with variable thickness of oxide, implanted with 185-keV O⁺ ions at 250 °C with a dose of $5 \times 10^{16} \text{ cm}^{-2}$: (1) 0 nm, (2) 50 nm, (3) 90 nm, (4) 140 nm, (5) 180 nm, and (6) 230 nm.

The above-mentioned features of RCs are in qualitative agreement with defect depth profile simulated by the MARLOWE code (Fig. 1, curve 1). The buried SiO₂ layer in the implanted SIMOX structure is situated in the region of positive strain. This region becomes invisible on the RC of SIMOX structure. Opposite to this case, the SiO₂ top layer of the SiO₂-Si structure is located in the region of high negative strain, and therefore the right shoulder of the RC shows a decreasing behavior (Fig. 2, curve 3). In this way we have strong evidence of the spatial separation of vacancy-type defects (negative strain) and interstitial-type defects (positive strain) in ion-implanted Si.

More detailed analysis was carried out by fitting of simulated x-ray spectra to the experimental RCs. X-ray scattering was calculated with a dynamical recursive formula approach.¹⁵ Ion-implanted Si crystal with continuously varying strain was conceived as a sum of thin slices with constant strain. The model of epitaxial heterostructure without misfit dislocations was used.¹⁵ A slice of negatively deformed Si was assumed as C_xSi_{1-x} crystal solid solution. The positive deformation was emulated by Ge_ySi_{1-y} crystal solid solution. The scattering amplitude of implanted Si differs from that of the used solid solutions. Nevertheless, interference features of graded strain crystal depend mainly on lattice deformation and only slightly on the scattering amplitude. We believe this model to be acceptable for our semiquantitative analysis.

The best-fitting simulated RC is shown in Fig. 2 (curve 1') and the corresponding strain depth profile is plotted in Fig. 1 (curve 1'). It should be noted that in the region of positive strain the best fitting was obtained at an exponentially decreasing strain with an *e*-times decreasing length of 10 nm. The fitted value of negative strain at undersurface region of implanted Si [$(\Delta d/d)_{\perp} \approx -1.3 \times 10^{-3}$] agrees satisfactorily with strain quantity, estimated in Ref. 13 for the case of 120 keV O⁺-ion implantation with a dose of $1 \times 10^{17} \text{ cm}^{-2}$ at elevated temperatures.

Three main differences between the defect profile, obtained as a result of fitting to the experimental RC, and the MARLOWE-code-simulated one (Fig. 1, curves 1' and 1, respectively) are as follows. (i) The region of fitted positive strain is distinctly narrower than the simulated one; (ii) The middle part of the implanted Si layer was determined as a nonstrained material where strains of opposite signs are completely intercompensated; and (iii) The near surface region of

high negative strain is deeper than the simulated one.

In summary, some characteristics of damage layers formed in Si during O⁺-ion implantation were simulated by the MARLOWE binary collision computer code. Simulated defect depth profile was compared with the strain distribution, obtained from fitting of modeled x-ray diffraction data to experimental RCs for Si, SIMOX, and SiO₂/Si structures implanted with high O⁺-ion dose at elevated temperature. The simulated depth profile of strain reasonably describes the experimental data. We attained strong evidence of spatial separation of vacancy-type defects (negative strain) and interstitial-type defects (positive strain) in ion-implanted silicon. The use of SIMOX and SiO₂-Si structures allowed to elucidate some characteristics of damage layers formed in Si at high-dose-ion implantation with elevated temperatures. These results can be used for optimizing implant conditions for SIMOX fabrication.

This work was partially supported by Conselho Nacional de Desenvolvimento Científico e Tecnológico do Brasil (CNPq) - Process No. 552056/02-2. The author (I.D.) would like to thank Dr. C.A. Cima for useful discussions.

- ¹J. P. Colinge, *Silicon-on-Insulator Technology: Materials to VLSI*, 2nd ed. (Kluwer, Boston, 1997).
- ²D. K. Sadana and J. P. de Souza, US Patent No 5,930,643.
- ³P. D. Townsend, J. C. Kelly, and N. E. W. Hartley, *Ion Implantation Sputtering and Their Applications* (Academic, London, 1976).
- ⁴*A Survey of Semiconductor Radiation Technique*, edited by L. S. Smirnov (Mir, Moscow, 1983).
- ⁵O. W. Holland, J. D. Budai, and B. Nielsen, *Mater. Sci. Eng., A* **253**, 240 (1998).
- ⁶S. Coffa, V. Privitera, F. Priolo, S. Libertino, and G. Mannino, *J. Appl. Phys.* **81**, 1639 (1997).
- ⁷R. Kalyanaraman, T. E. Haynes, O. W. Holland, and G. H. Gilmer, *J. Appl. Phys.* **91**, 6325 (2002).
- ⁸P. Pellegrino, P. Leveque, J. Wong-Leung, C. Jagadish, and B. G. Svensson, *Appl. Phys. Lett.* **78**, 3442 (2001).
- ⁹N. Yarykin, *Appl. Phys. Lett.* **80**, 1492 (2002).
- ¹⁰P. Pellegrino, P. Leveque, H. Kortegaard-Nielsen, J. Wong-Leung, C. Jagadish, and B. G. Svensson, *Appl. Phys. Lett.* **80**, 1494 (2002).
- ¹¹M. T. Robinson and I. M. Torrens, *Phys. Rev. B* **9**, 5008 (1974).
- ¹²M. T. Robinson, *Nucl. Instrum. Methods Phys. Res. B* **40**, 10717 (1989).
- ¹³J. P. de Souza, Yu. Suprun-Belevich, H. Boudinov, and C. A. Cima, *J. Appl. Phys.* **87**, 8385 (2000).
- ¹⁴J. P. de Souza, Yu. Suprun-Belevich, H. Boudinov, and C. A. Cima, *J. Appl. Phys.* **89**, 42 (2001).
- ¹⁵P. F. Fewster, *X-Ray Scattering from Semiconductors* (Imperial College Press, London, 2000).